



ELSEVIER

Available online at www.sciencedirect.com

ScienceDirect

Tetrahedron 62 (2006) 10647–10659

Tetrahedron

A comparative mechanistic analysis of the stereoselectivity trends observed in the oxidation of chiral oxazolidinone-functionalized enecarbamates by singlet oxygen, ozone, and triazolinedione

J. Sivaguru,^a Thomas Poon,^b Catherine Hooper,^b Hideaki Saito,^{a,c,d} Marissa R. Solomon,^a Steffen Jockusch,^a Waldemar Adam,^{e,f} Yoshihisa Inoue^{c,d} and Nicholas J. Turro^{a,g,*}

^aThe Department of Chemistry, Columbia University, New York, NY 10027, USA

^bJoint Science Department, W.M. Keck Science Center, 925 N. Mills Ave., Claremont McKenna, Pitzer, and Scripps Colleges, Claremont, CA 91711, USA

^cThe Department of Applied Chemistry, Osaka University, 2-1 Yamada-oka, Suita 565-0871, Japan

^dThe Entropy Control Project, ICORP, JST, 4-6-3 Kamishinden, Toyonaka 560-0085, Japan

^eInstitute für Organische Chemie, Universität Würzburg, D-97074 Würzburg, Germany

^fThe Department of Chemistry, University of Puerto Rico, Facundo Bueso 110, Rio Piedras, PR 00931, USA

^gThe Department of Chemical Engineering, Columbia University, New York, NY 10027, USA

Received 30 May 2006; revised 26 July 2006; accepted 31 July 2006

Available online 29 September 2006

Abstract—The stereoselectivity in the reactions of the *E/Z* enecarbamates **1**, equipped with the oxazolidinone chiral auxiliary, has been examined for singlet oxygen (¹O₂), ozone (O₃), and 4-phenyl-1,2,4-triazoline-3,5-dione (PTAD) in a variety of solvents as a function of temperature. The oxidative cleavage of the alkenyl functionality by ¹O₂ and O₃ releases the enantiomerically enriched methyldeoxybenzoin (MDB) product. The *extent* (% ee) as well as the *sense* (*R* vs *S*) of the stereoselectivity in the MDB formation depends on the electronic nature of the oxidant. A high stereoselectivity, substantially dependent on solvent and temperature, is displayed for the reactions with ¹O₂, whereas the ground-state reactants O₃ and PTAD are rather unaffected by solvent and temperature variations. The present comparative analysis clearly substantiates our hypothesis of stereoselective vibrational quenching of the attacking ¹O₂, whereas O₃ and PTAD are only subject to steric impositions. The electronically excited ¹O₂ is sensitive to all three stereochemically relevant structural characteristics embodied in the chiral enecarbamates, namely the *R/S* configuration at the C₄ position of the oxazolidinone chiral auxiliary, the *Z/E* geometry of the ‘alkene’ functionality, and *R/S* configuration at the C₃’ position of the enecarbamate side chain.

© 2006 Elsevier Ltd. All rights reserved.

1. Introduction

High enantioselectivity in photochemical reactions^{1–3} depends on effective manipulation of chiral/prochiral faces of the reactant within the short lifetimes of the excited states.⁴ To imprint stereocontrol in the photoproduct, confined media^{5–10} has been employed with considerable success; however, to obtain a high enantioselectivity in solution still constitutes a formidable challenge.^{1–3} In this regard, a novel concept, which we have explored in the stereoselective photooxidative cleavage of chiral enecarbamates, involves selective deactivation (quenching) of one of the diastereomers in a pair of chiral excited states.^{11–13} To demonstrate this concept, we have compared the reaction of enecarbamates **1**

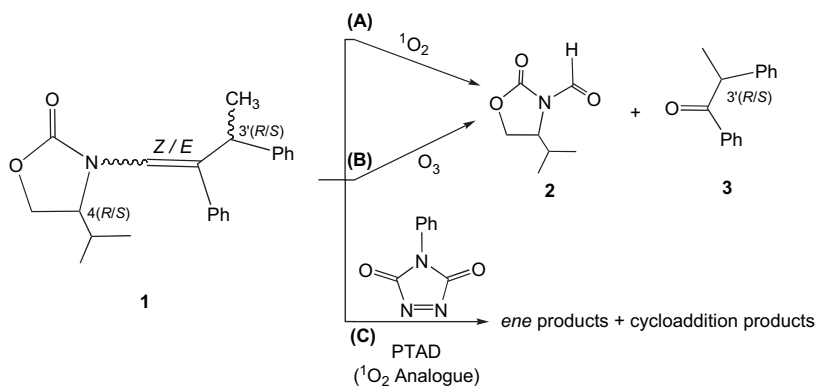
(Scheme 1) with related reactive species viz. singlet oxygen (¹O₂),^{14–17} ozone (O₃),¹⁸ and 4-phenyl-1,2,4-triazoline-3,5-dione (PTAD).^{19–23} Indeed, the high stereoselectivity was observed in the formation of the product MDB **3** (Scheme 1) in the reactions with ¹O₂. The observed high stereoselectivity was hypothesized to result from a combination of steric interactions and selective deactivations of the excited state (Scheme 1).^{11,24}

Previously we have shown^{24–26} that the photooxidation of enecarbamates by ¹O₂ leads to diastereomerically pure dioxetanes (complete conversion), as exemplified for the chiral *Z*-configured enecarbamate 1'*Z*,4*R*(*iPr*),3'(R/S)-**1** (Fig. 1).

The salient reactivity feature in the exposed snapshot in Figure 1 is the approach of ¹O₂ on to the double bond, where in addition to the steric hindrance imposed on the ¹O₂, the possible synergistic stereoselective vibrational quenching

Keywords: Kinetic resolution; Ozonolysis; Photooxygenation; Substituent; Solvent and temperature effects; Vibrational quenching.

* Corresponding author. Tel.: +1 212 854 2175; fax: +1 212 932 1289; e-mail: njt3@columbia.edu



Scheme 1. Reactions of oxazolidinone-functionalized *Z/E*-encarbamates **1** with (A) $^1\text{O}_2$, (B) O_3 , and (C) PTAD.

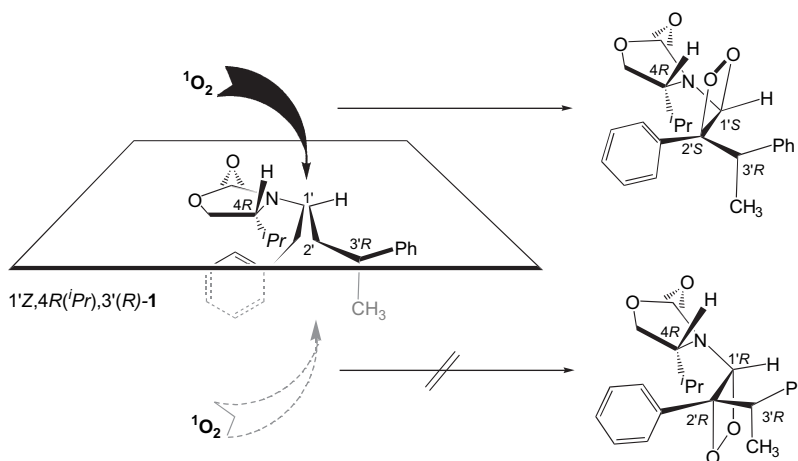


Figure 1. Preferred π -facial attack of $^1\text{O}_2$ from above, controlled by the steric shielding of the 4-isopropyl substituent of the oxazolidinone chiral auxiliary in *Z* encarbamates.

of the $^1\text{O}_2$ from the bottom face could dictate the observed high diastereoselectivity. Moreover, the stereoselection in the dioxetane formation is independent from the configuration of the alkyl side chain at the $\text{C}_{3'}$ position and the size of the alkyl substituent at the C_4 position (*Me*, *iPr*, *Ph*) of the oxazolidinone chiral auxiliary.^{24–26} For example, the diastereomer **1'Z,4*R*(*iPr*),3'(*R*)-1** (Fig. 1) that possesses the *R* configuration at the C_4 position affords the corresponding [**1'S,2'S**] dioxetane with complete stereocontrol [diastereomeric ratios (d.r.) of >95:5]. Further, the stereoselection in the MDB product **3** (Scheme 1) upon photooxidative cleavage of these oxazolidinone-functionalized encarbamates by $^1\text{O}_2$ depends not only on the alkene geometry (*Z/E*), the size of the C_4 alkyl substituent (*H*, *Me*, *iPr*) in the oxazolidinone ring, and the configuration (*R/S*) at the $\text{C}_{3'}$ stereogenic center of the phenethyl side chain, but also on the nature of the solvent and the reaction temperature.^{11,27} The stereoselectivity of oxidation of the conformationally more flexible *E* diastereomer responds sensitively to such reaction conditions (ee values of up to 97%), whereas the conformationally more rigid *Z* diastereomer behaves less sensitively to such manipulation (ee values of up to 30%).^{11,27} We proposed that conformational effects (entropy control) are responsible for stereoselective quenching of $^1\text{O}_2$ by vibrational deactivation (a new concept!), in concert with the steric interactions leading to stereoselective oxidative cleavage of the double bond by the attacking $^1\text{O}_2$.^{11,27}

In the present work, we compare the reactivity of singlet oxygen ($^1\text{O}_2$, Scheme 1A) for both *E* and *Z* diastereomers of the encarbamates (Chart 1) with O_3 , an electrophilic oxidant akin to $^1\text{O}_2$ (Scheme 1B) and PTAD, a ground-state analogue of $^1\text{O}_2$ (Scheme 1C). If, indeed, our hypothesis of stereoselective vibrational quenching in the photooxidative cleavage of the encarbamates by $^1\text{O}_2$ proves to be correct, then PTAD would constitute a good test reagent, as it is considered analogous^{19–23} in its chemical reactivity to $^1\text{O}_2$, but as a ground-state molecule PTAD, is not subject to vibrational deactivation.²⁸ Moreover, in view of its much larger size than $^1\text{O}_2$, this bulkier species would be more sensitive to steric effects. Similarly, the highly reactive O_3 oxidant is also a ground-state species and is not subjected to vibrational quenching as in the case of $^1\text{O}_2$. Thus, the electrophilic O_3 , a highly reactive ground-state oxidant would provide an opportunity to probe the importance of the excited-state character in the photooxygenation process. An additional advantage of O_3 over PTAD is the fact that like $^1\text{O}_2$, oxidation of both *Z* and *E* encarbamates **1** by O_3 affords the same MDB product **3**,²⁹ which should facilitate the direct comparison of the stereoselection of these two oxidants.

In the present work, analogous to previous reports,^{11,27} we shall employ both *E* and *Z* oxazolidinone-functionalized encarbamates as 50:50 diastereomeric mixtures of the *R/S* isomers at the $\text{C}_{3'}$ position. Thus, for the purpose of this

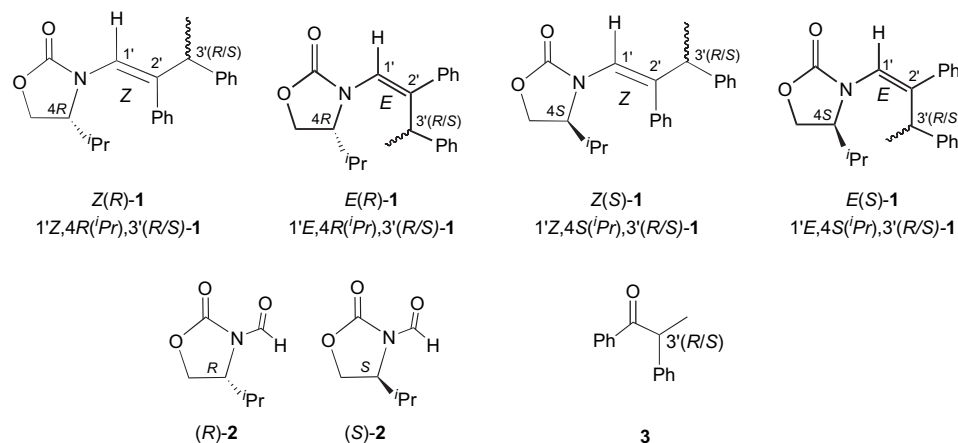


Chart 1. Structure matrix.

study, stereoselectivity will be defined as selective consumption (kinetic resolution) of enecarbamaes (upon reaction with $^1\text{O}_2$, O_3 , and PTAD) based upon the $\text{C}_{3'}$ stereochemistry.¹¹ The chemical reactivity of $^1\text{O}_2$, O_3 , and PTAD toward the diastereomeric enecarbamaes shall be examined as a function of (i) *E/Z* alkene geometry, (ii) the *R/S* configuration at the C_4 position of the oxazolidinone chiral auxiliary, (iii) the *R/S* configuration of the alkyl substituent at the $\text{C}_{3'}$ position of the oxazolidinone chiral auxiliary, (iv) the solvent, and (v) the reaction temperature. The stereoselectivity for the reactions with PTAD^{19–23} (vs $^1\text{O}_2$) is based on the comparison of diastereomeric composition of the enecarbamaes **1** before and after the reaction. On the other hand, for the comparison of $^1\text{O}_2$ with O_3 , the enantiomeric excess in the MDB product **3** was examined (Scheme 1).²⁹

Herein we report the results of an extensive investigation, which for the first time compares the stereochemical behavior of such chemically diverse reactive species ($^1\text{O}_2$, O_3 , and PTAD), whose reactivity are analogous in their reaction with the diastereomeric *E* and *Z* enecarbamaes **1**. Evidently, the observed difference in the stereocontrol of these reactive species validates our hypothesis of significant vibrational deactivation (physical quenching) of the electronically excited $^1\text{O}_2$ as a factor for the observed stereoselectivity in the formation of the MDB product. Such selective quenching of diastereomeric excited states constitute a promising *stereochemical tool* to effect enantioselective photoreactions.

2. Experimental

2.1. Materials

All regular solvents were purchased from Aldrich and the deuterated solvents from Cambridge Isotope Labs and used as received. CDCl_3 was stored over sodium bicarbonate prior to use. Flash chromatography was carried out on silica gel, while 2-mm thick silica-gel plates (EMD 60F) were employed for preparative TLC. Commercially available compounds were purified by standard procedures. The *Z* and *E* enecarbamaes were synthesized by previously published methods.^{11,12,24–26} The *Z* and *E* enecarbamaes **1** were used as 50:50 mixture of *R* and *S* enantiomers at the $\text{C}_{3'}$ position (Chart 1), but the epimeric pair is optically pure at the

C_4 stereogenic center of the oxazolidinone chiral auxiliary. O_3 was generated by means of an OL100 Ozone Generator.

2.2. Instrumentation

GC analyses were carried out on a Varian 3900 gas chromatograph, equipped with an auto-sampler. A Varian Factor-4 VG-1ms column ($l=25$ m, $id=0.25$ mm, $df=0.25$ μm) was employed for the separation on the achiral stationary phase, with a program of 50 $^\circ\text{C}$ for 4 min, raised to 225 $^\circ\text{C}$ at 10 $^\circ\text{C}/\text{min}$, and kept at 225 $^\circ\text{C}$ for 10 min. A Varian CP-Chirasil-DEX CB column ($l=25$ m, $id=0.25$ mm, $df=0.25$ μm) was used for the separations on the chiral stationary phase, with a program of 135 $^\circ\text{C}$ for 70 min, raised to 200 $^\circ\text{C}$ at 15 $^\circ\text{C}/\text{min}$, and kept at 200 $^\circ\text{C}$ for 30 min. The ^1H NMR and ^{13}C NMR spectra were recorded on BRUKER spectrometers (Model DPX300 or DRX300). For the reaction with PTAD, all ^1H NMR spectra were obtained in CDCl_3 on an AC360 Bruker spectrometer, supplied with NTNMR software version 1.3 and processed with Mestre-C 4.1.1.0.

2.3. Photooxygenation of *Z* and *E* enecarbamaes

The appropriate *Z* or *E* enecarbamate epimeric pair **1** (see Chart 1) and the methylene blue sensitizer were dissolved in 0.7 mL of the desired deuterated solvent (the enecarbamate concentration was 3.0×10^{-3} M and that of methylene blue 3.7×10^{-4} M), placed into the NMR tube, sealed with a rubber septum, fitted with a gas delivery needle, and a vent needle. Dry O_2 gas was purged through the sample for 20 min, while irradiating with a 500-W halogen lamp, equipped with a cutoff filter (<500 nm). After irradiation, the samples were submitted to ^1H NMR spectroscopy to determine the conversion (kept below 50%). The mass balance (based on unreacted enecarbamate and formed MDB product) and the conversion (based on unreacted enecarbamate) were determined by GC analysis on an achiral stationary phase, with 4,4'-di-*tert*-butylbiphenyl as calibration standard. The enantioselectivity (% ee) of the MDB product was determined by GC analysis on a chiral stationary phase.

2.4. Reaction of enecarbamaes with PTAD

The respective enecarbamate pair (0.013 mmol) in CDCl_3 was placed in the NMR tube followed by the addition of

0.003 mmol of the PTAD dissolved in chloroform-*d*. The amount of PTAD was chosen to give a maximum of 25% conversion. The reaction was allowed to proceed at 24, 7, or $-20\text{ }^{\circ}\text{C}$ until the disappearance of the characteristic red color of the PTAD indicated that the reaction had terminated. The samples were then subjected to ^1H NMR spectroscopy to record the conversion and diastereomeric excess.

2.5. General procedure for the ozone oxidation of the enecarbamates

An aliquot of the appropriate enecarbamate epimeric pair was taken from a standard solution in dichloromethane and transferred to a NMR tube. Most of the solvent was removed by means of a gentle stream of N_2 , the residual solvent removed by placing the open NMR tube into a vacuum (~ 12 in. Hg) oven at room temperature for at least 2 h. To each NMR tube was added 0.7 mL of the desired deuterated solvent. The NMR tube with the enecarbamate was kept in a cooling bath at the required temperature. A separate test tube with the deuterated solvent of interest was placed into the cooling bath at the required temperature, and saturated with O_3 (generated by OL100 Ozone Generator) by purging with O_3 gas for a minimum of 15–20 min. The required amount of an O_3 -saturated solution was added to the NMR tube and the conversion monitored by ^1H NMR spectroscopy (conversion $<20\%$). The amounts of O_3 -saturated solution used in the case of $\text{CD}_2\text{Cl}_2/\text{CDCl}_3$ were 50 μL at $+20\text{ }^{\circ}\text{C}$, 40 μL at $-15\text{ }^{\circ}\text{C}$, 30 μL at $-45\text{ }^{\circ}\text{C}$, and 25 μL at $-70\text{ }^{\circ}\text{C}$. For CD_3OD , the amounts of O_3 -saturated solution were 90 μL at $+20\text{ }^{\circ}\text{C}$, 50 μL at $-15\text{ }^{\circ}\text{C}$, 40 μL at $-45\text{ }^{\circ}\text{C}$, and 35 μL at $-70\text{ }^{\circ}\text{C}$. Because of the lower solubility of ozone in CD_3OD ,³⁰ larger amounts of O_3 -saturated solution were used in the CD_3OD experiments. After addition of the O_3 , the reaction was allowed to proceed at the desired temperature for 15 min, and then analyzed by ^1H NMR spectroscopy, with conversion calculated by integration of the aldehyde (decomposition product) and the unreacted enecarbamates signals. The samples were then subjected to GC analysis on a chiral stationary phase.

2.6. General procedure for the oxidation of the enecarbamates by triphenyl phosphite ozonide

A 0.5 mL aliquot of triphenyl phosphite (1.72×10^{-6} M) in dichloromethane was pipetted into a colorless 1-dram vial, and placed into a cooling bath kept at $-70\text{ }^{\circ}\text{C}$. The O_3 gas was bubbled through the chilled solution for a minimum of 10 min until the solution acquired the characteristic purple color of O_3 saturation (O_3 generated by OL100 Ozone Generator), followed by N_2 gas to remove excess O_3 (ca. 5 min). To the colorless triphenyl phosphite ozonide solution was added a pre-cooled solution (kept in the same cooling bath) of *Z(R)*-**1** in dichloromethane, and the mixture was allowed to react for 40 min in the cooling bath at $-70\text{ }^{\circ}\text{C}$. After 40 min, the vial was removed from the cooling bath and the contents allowed to warm up to room temperature (ca. $20\text{ }^{\circ}\text{C}$). The reaction mixture was concentrated and submitted to GC analysis on a chiral and an achiral stationary phase, with di-*tert*-butylbiphenyl as calibration standard.

3. Results

The reaction between the chiral enecarbamates **1** and the three different reactive species $^1\text{O}_2$, O_3 , and PTAD was carried out to assess the difference in their reactivity and stereoselectivity. The Evans chiral auxiliary^{31–33} in the enecarbamate diastereomer *Z*-**1** serves as the essential stereochemical director, whereas the 1-phenylethyl substituent at the C_3' position of the double bond minimizes the *ene* reaction during photooxygenation^{24–26} as the required coplanar alignment of the only allylic hydrogen atom is encumbered. The *E*-**1** enecarbamate was prepared from the *Z*-**1** diastereomer by direct or sensitized photochemical isomerization,³⁴ followed by chromatographic separation. Photooxygenation of the enecarbamate **1** gave quantitatively the expected oxazolidinone aldehyde **2** and the chiral methyldeoxybenzoin (MDB) **3** on complete conversion of the substrate. In previous experiments,^{24–26} the thermally labile dioxetane was detected at $-35\text{ }^{\circ}\text{C}$ and shown to decompose readily at room temperature (ca. $20\text{ }^{\circ}\text{C}$) into aldehyde **2** and MDB **3** (Scheme 1, Chart 1).

The reactivity of chiral *Z* and *E* enecarbamates **1** with $^1\text{O}_2$, O_3 , and PTAD, was compared by examining the selectivity observed with the three different reactants. The product studies for the reactions of *Z* and *E* enecarbamates **1** with PTAD^{19–23} are presented in Table 1. The comparable results for reactions with O_3 ²⁹ and $^1\text{O}_2$,^{11,27} which have been previously published are summarized in Tables 2 and 3, respectively. The reactions with PTAD as with the previous work, employed a 50:50 mixture of C_3' epimers and were conducted to conversions less than 25% to minimize formation of side products.

Examination of Table 1 shows that there is no significant effect of the alkene geometry in the PTAD reaction with the chiral *Z* and *E* enecarbamates **1**. As exemplified in Entry 1 of Table 1, the addition of PTAD to *E(R)*-**1** in CDCl_3 at $24\text{ }^{\circ}\text{C}$ accumulated a 14% diastereomeric excess of the

Table 1. Diastereomeric excess in enecarbamate **1** after reaction with PTAD in CDCl_3

Entry	Enecarbamate ^a	Temp ($^{\circ}\text{C}$)	% de enecarbamate ^{b-d}	% Conv ^c
1	<i>E(R)</i> - 1	24	14 [$\text{C}_3'\text{S}$]	17
2		7	8 [$\text{C}_3'\text{S}$]	20
3		-20	11 [$\text{C}_3'\text{S}$]	16
4	<i>E(S)</i> - 1	24	13 [$\text{C}_3'\text{R}$]	13
5		7	10 [$\text{C}_3'\text{R}$]	11
6	<i>Z(R)</i> - 1	24	10 [$\text{C}_3'\text{S}$]	19
7		7	13 [$\text{C}_3'\text{S}$]	13
8		-20	14 [$\text{C}_3'\text{S}$]	19
9	<i>Z(S)</i> - 1	24	0	16
10		7	4 [$\text{C}_3'\text{R}$]	13
11		-20	4 [$\text{C}_3'\text{R}$]	18

^a A ca. 50:50 mixture of diastereomers (total concentration 0.1 M) was used.

^b Average of three runs (error $\pm 4\%$).

^c Conversion was monitored by ^1H NMR spectroscopy; the conversion (error $\pm 3\%$) was kept low to prevent side reactions.^{19–23}

^d It is important to note that the C_3' isomer of the enecarbamate substrate is observed in excess in the product mixture, since it is the less reactive epimer of the starting enecarbamate pair; for example, in entry 1, PTAD is relatively more reactive with the $\text{C}_3'(\text{R})$ epimer and, hence, the $\text{C}_3'(\text{S})$ epimer of *E(R)*-**1** accumulates.

Table 2. Determination of the stereoselectivity factor (*s*) for the formation of (*R/S*)-MDB product in the oxidation^a of **1** by O₃ as a function of solvent and temperature²⁹

Entry	Enecarbamate ^a	Solvent	Temp (°C)	% ee MDB ^b	% Conv ^c	<i>s</i> ^d	$\Delta\Delta H^\ddagger$ (kcal mol ⁻¹) ^d	$\Delta\Delta S^\ddagger$ (cal mol ⁻¹ K ⁻¹) ^d
1	<i>E(R)</i> - 1	CD ₂ Cl ₂	20	22 (<i>S</i>)	6	1.6	0.16	1.49
2			-15	24 (<i>S</i>)	15	1.7		
3			-45	16 (<i>S</i>)	18	1.4		
4			-70	18 (<i>S</i>)	27	1.5		
5	<i>E(R)</i> - 1	CDCl ₃	20	18 (<i>S</i>)	12	1.5	-0.48	-0.97
6			-15	20 (<i>S</i>)	17	1.6		
7			-70	29 (<i>S</i>)	25	2.0		
8	<i>E(R)</i> - 1	CD ₃ OD	20	4 (<i>S</i>)	4	1.1	0.12	0.16
9			-15	2 (<i>S</i>)	6	1.1		
10			-45	0	4	1.0		
11			-70	4 (<i>S</i>)	5	1.1		
12	<i>Z(R)</i> - 1	CD ₂ Cl ₂	20	31 (<i>R</i>)	10	2.0	-0.14	0.79
13			-15	30 (<i>R</i>)	12	1.9		
14			-78	36 (<i>R</i>)	9	2.2		
15	<i>Z(S)</i> - 1	CD ₂ Cl ₂	20	33 (<i>S</i>)	6	2.0	0.6	2.98
16			20	27 (<i>S</i>)	9	1.8		
17			-15	38 (<i>S</i>)	7	2.3		
18			-15	12 (<i>S</i>)	20	1.3		
19			-45	6 (<i>S</i>)	27	1.2		
20			-70	36 (<i>S</i>)	9	2.2		
21			-70	4 (<i>S</i>)	36	1.1		
22	<i>Z(S)</i> - 1	CDCl ₃	20	20 (<i>S</i>)	16	1.6	0.08	1.03
23			-15	16 (<i>S</i>)	17	1.4		
24			-70	18 (<i>S</i>)	14	1.5		
25	<i>Z(S)</i> - 1	CD ₃ OD	20	20 (<i>S</i>)	3	1.5	-0.05	0.62
26			-15	21 (<i>S</i>)	4	1.5		
27			-45	22 (<i>S</i>)	16	1.6		
28			-70	22 (<i>S</i>)	7	1.6		

^a A 50:50 mixture of diastereomers (total concentration 2.3 × 10⁻³ M) was used.^b Average of three runs (error ±6%).^c Conversion monitored by ¹H NMR spectroscopy the conversion was kept low to prevent side reactions.¹⁸^d Calculated from Eqs. 1–3.**Table 3.** Determination of the stereoselectivity factor (*s*) for the formation of (*R/S*)-MDB product in the photooxygenation^a of **1** as a function of solvent and temperature^{11,27}

Entry	Enecarbamate ^a	Solvent	Temp (°C)	MDB ^b (% ee)	Conv ^c (%)	<i>s</i> ^d	$\Delta\Delta H^\ddagger$ (kcal mol ⁻¹) ^d	$\Delta\Delta S^\ddagger$ (cal mol ⁻¹ K ⁻¹) ^d
1	<i>E(R)</i> - 1	CDCl ₃	50	8 (<i>S</i>)	5	1.2	-4.5	-14
2			18	63 (<i>R</i>)	17	5		
3			-15	78 (<i>R</i>)	37	13		
4			-40	88 (<i>R</i>)	43	31		
5	<i>E(R)</i> - 1	CD ₂ Cl ₂	20	34 (<i>S</i>)	25	2.3	-4.0	-15
6			-20	27 (<i>R</i>)	65	2.7		
7			-60	82 (<i>R</i>)	54	40		
8	<i>E(R)</i> - 1	CD ₃ CN	50	64 (<i>S</i>)	23	5.5	-4.5	-17
9			18	30 (<i>S</i>)	34	2.1		
10			-15	0	28	1.0		
11			-40	58 (<i>R</i>)	37	5.2		
12	<i>E(R)</i> - 1	CD ₃ OD	50	70 (<i>R</i>)	30	7.6	-2.5	-4.9
13			18	85 (<i>R</i>)	34	19		
14			-15	90 (<i>R</i>)	17	23		
15			-40	94 (<i>R</i>)	12	37		
16			-70	97 (<i>R</i>)	8	72		
17	<i>E(S)</i> - 1	CD ₂ Cl ₂	20	28 (<i>R</i>)	29	2.0	5.3	19.0
18			-20	36 (<i>S</i>)	59	3.4		
19			-60	88 (<i>S</i>)	56	45		
20	<i>Z(R)</i> - 1	CD ₂ Cl ₂	20	22 (<i>R</i>)	29	1.7	-0.7	1.2
21			-20	22 (<i>R</i>)	59	2.1		
22			-60	30 (<i>R</i>)	56	2.6		

^a The *E* enecarbamate concentration is 3.0 × 10⁻³ M and that for the methylene blue sensitizer is 3.7 × 10⁻⁴ M.^b Determined by GC analysis on a chiral stationary phase.^c Conversion (convn) of enecarbamates determined by GC analysis on an achiral stationary phase with 4,4'-di-*tert*-butylbiphenyl as calibration standard, and by ¹H NMR spectroscopy; averages of three runs, within 5% error of the stated values.^d Calculated from Eqs. 1–3.

C_3 -(*S*)-epimer of $E(R)$ -**1** after the reaction; thus, the C_3 -(*R*)-epimer of $E(R)$ -**1** is more reactive. By changing the alkene geometry to the *Z* enecarbamate, the C_3 -(*S*)-epimer of $Z(R)$ -**1** accumulated in a 10% diastereomeric excess under identical conditions (Entry 6), which indicates that the C_3 -(*R*)-epimer of $Z(R)$ -**1** is more reactive. Thus, when the *R* configuration at the C_4 position of the oxazolidinone chiral auxiliary was used, the C_3 -(*R*)-epimer was more reactive irrespective of the alkene *Z/E* geometry. For example (Table 1; Entries 1–3), PTAD is more reactive for the C_3 -(*R*)-epimer of $E(R)$ -**1** and, hence, the C_3 -(*S*)-epimer of $E(R)$ -**1** was observed in excess after the reaction. Similarly, PTAD is more reactive for the C_3 -(*R*)-epimer of $Z(R)$ -**1** and, thus, the C_3 -(*S*)-epimer of $Z(R)$ -**1** results in excess (Table 1; Entries 6–8). The low selectivity observed in the reaction (<15%) indicates that the C_3 stereocenter is not playing a dominant role. Since the sense in the stereoselection was reversed upon changing the configuration at the C_4 position of the oxazolidinone chiral auxiliary from *R* to *S* (Table 1; Entries 4,5 and 9–11), the PTAD reaction is well behaved.

The enantiomeric excesses in the MDB product upon oxidative cleavage of the epimeric pairs of oxazolidinone-derived *E* and *Z* enecarbamates by O_3 are given in Table 2 for three different solvents (CD_2Cl_2 , $CDCl_3$, and CD_3OD) and at various temperatures. The conversion was kept low to avoid side reactions¹⁸ and the enantiomeric excess (ee) was obtained by GC analysis of the methyldeoxybenzoin (MDB) product on a chiral stationary phase. Inspection of Table 2 reveals the following features: (i) The same MDB enantiomer is formed preferentially irrespective of the solvent, that is, employed, but the ee values for both *E* and *Z* enecarbamates change notably, when compared at the same temperature; for example, the ee value for the O_3 oxidation of $E(R)$ -**1** in CD_2Cl_2 is 18% (Entry 4), in $CDCl_3$ it is 29% (Entry 7), and in CD_3OD it is 4% (Entry 11) at -70 °C. (ii) The sense of the preferentially generated MDB enantiomer depends on the configuration at the C_4 position of the oxazolidinone ring, as well as the alkene *Z/E* geometry; for example, $E(R)$ -**1** substrate gave the *S*-MDB product in excess, whereas the corresponding $Z(R)$ -**1** enecarbamate afforded *R*-MDB in excess. (iii) The same MDB enantiomer is produced irrespective of the temperature. (iv) The change in the configuration at the C_4 position of the oxazolidinone reverses the sense of the MDB enantiomer to the same extent, which indicates that the O_3 oxidation is also well behaved. (v) The observed ee values depend on the extent of conversion; thus, the ee values were moderate at low conversions and small at high conversions.

The stereoselectivity factor (*s*), which represents the ratio of the rates of formation (k_R/k_S) of the enantiomeric products, may be computed from the observed ee values at a given conversion by means of Eqs. 1 and 2.^{35–38} The computed *s* values for the O_3 oxidation are given in Table 2, and are quite low, i.e., at best ~2. Consequently, the stereocontrol in the ozonolysis reaction is relatively poor.

$$s = \frac{k_R}{k_S} = \frac{\ln[1 - C(1 + ee_{MDB})]}{\ln[1 - C(1 - ee_{MDB})]} \quad (1)$$

where *C* is the conversion and ee_{MDB} the ee value of the MDB product

$$\ln(k_R/k_S) = \ln[(100 + \% ee)/(100 - \% ee)] \quad (2)$$

$$\begin{aligned} -\Delta\Delta G^\ddagger_{R-S}/RT &= \ln(k_R/k_S) \\ &= \Delta\Delta S^\ddagger_{R-S}/R - \Delta\Delta H^\ddagger_{R-S}/RT \end{aligned} \quad (3)$$

The effect of the solvent type and polarity was examined by conducting the ozonolysis in the polar, protic solvent CD_3OD , and the low-polarity halogenated solvents CD_2Cl_2 and $CDCl_3$. For the oxidative cleavage of the $E(R)$ -**1** substrate by O_3 , the solvent dependence of the stereoselectivity follows the order (the ee values are given in parentheses) CD_3OD (4%) < $CDCl_3$ (18%) < CD_2Cl_2 (22%) at the common temperature of about 20 °C (Table 2; Entries 8, 5, and 1). Similarly, for the O_3 cleavage of the *Z* isomer [$Z(S)$ -**1**], the solvent dependence of the stereoselectivity follows the order CD_3OD (20%) \approx $CDCl_3$ (20%) < CD_2Cl_2 (33%), also at about 20 °C (Table 2; Entries 25, 22, and 15). Evidently, the best diastereoselectivity is obtained for CD_2Cl_2 , whereas the lowest stereocontrol is displayed by the hydrogen-bonded solvent methanol at the same temperature. Since the stereoselectivity in $CDCl_3$ and CD_3OD is similar (Table 2; compare Entries 22–24 and 25–28), the solvent polarity alone cannot be the responsible factor for the stereocontrol in the oxidative cleavage of the $Z(S)$ -**1** enecarbamates by O_3 .

In contrast, the ozonolysis of the $E(R)$ -**1** diastereomer in $CDCl_3$ and CD_3OD displays significant differences in the observed stereoselectivity (Table 2; compare Entries 5–7 and 8–11). Although not as dramatic as observed for the 1O_2 oxidation, the effect is attributed to the differing alkene geometry (*Z* vs *E* enecarbamate) and the various conformations that these diastereomers may adopt in the two solvents.^{11,27,29} To be noted is the comparatively high ee values for the *Z* versus the *E* enecarbamates. Mechanistically most revealing is the finding that the *R*-MDB enantiomer is the favored product for $Z(R)$ -**1** (Table 2; Entries 12–14), but the *S*-MDB isomer dominates for $E(R)$ -**1** (Table 2; Entries 1–11). For example, in CD_2Cl_2 at 20 °C $E(R)$ -**1** favors the *S*-MDB product (Table 2; Entry 1), whereas $Z(R)$ -**1** prefers the *R*-MDB (Table 2; Entry 12) under the identical conditions.

Our previous results on the photooxygenation of *Z* and *E* enecarbamate (Table 3) showed that there is negligible effect of the alkyl substituent (methyl or isopropyl group) at the oxazolidinone C_4 position.^{11–13,24–27} Further, upon employing *R* or *S* antipodes at the C_4 position (Table 3), the sense of the enantioselectivity in the MDB product is reversed, while the extent of the stereocontrol in the photooxidative cleavage of the *E* enecarbamates is the same (within the experimental error). This is clearly displayed by the % ee data for the $E(R)$ -**1** and $E(S)$ -**1** diastereomers, as exemplified by their photooxygenation in CD_2Cl_2 at 20 °C (*s* factor ca. 2 for both; Entries 5 and 17 in Table 3). Thus, $E(R)$ -**1** (Table 3; Entries 5–7) favors the *S*-MDB enantiomer (34% ee at 25% convn), whereas $E(S)$ -**1** (Entries 17–19) favors the *R*-MDB (28% ee at 29% convn) enantiomer as the final oxidation products; the reversal in the enantioselectivity sense is expected.

The effect of the solvent type and polarity was examined by conducting the photooxygenation in the polar, aprotic solvent CD_3CN , the polar, protic solvent CD_3OD , and the

low-polarity halogenated solvents CD_2Cl_2 and CDCl_3 . For the photooxidative cleavage of the *E*-**1** substrate, the solvent dependence of the diastereoselectivity follows the order CD_3CN (30%) $\sim\text{CD}_2\text{Cl}_2$ (34%) $<\text{CDCl}_3$ (63%) $<\text{CD}_3\text{OD}$ (85%) at the common temperature of about 18–20 °C (Table 3; Entries 9, 5, 2, and 13); the ee values are given in parentheses. Evidently, the best stereoselectivity is obtained for the hydrogen-bonding solvent methanol (Table 3; Entry 13), whereas the lowest stereoselectivity is displayed by the aprotic acetonitrile (Table 3; Entry 9) at the same temperature of 18 °C. To be noted is the relatively high ee value in chloroform-*d* (Table 3; Entries 1–4). Again, mechanistically most revealing is the finding that the *R*-MDB enantiomer is the favored product in CDCl_3 and CD_3OD (Table 3; Entries 2 and 13), but the *S*-MDB isomer dominates in CD_2Cl_2 and CD_3CN (Table 3; Entries 5 and 9). Thus, also for the photooxidative cleavage of the *E(R)*-**1** enecarbamates, the stereoselectivity cannot be attributed to the solvent polarity alone.

Still more intriguing for mechanistic considerations is the temperature dependence of the ee values upon photooxygenation of the *E(R)*-**1** substrate (Table 3). Only in methanol is the extent of the diastereoselectivity relatively constant (note the high ee value of 97% at –70 °C, i.e., nearly perfect stereocontrol!); moreover, the same enantiomer, namely *R*-MDB, is formed over the entire temperature range from –70 to +50 °C (Table 3; Entries 12–16). In the other solvents, a temperature-dependent change in the sense of stereoselection is observed from the usual *R*-MDB to the *S*-MDB isomer. For example, very good stereocontrol (ee value of 88%) in favor of *R*-MDB is found in chloroform-*d* at –40 °C (Table 3; Entry 4), but the *S*-MDB isomer is favored with only poor diastereoselectivity (ee value of only 8%) at +50 °C (Table 3; Entry 1). This inflection in the enantioselectivity sense (*R* to *S* isomer) occurs in CDCl_3 above +18 °C (Table 3; Entries 1 and 2), whereas in CD_2Cl_2 it takes place between +20 and –20 °C (Table 3; Entries 5 and 6). In the case of CD_3CN , the change in the sense takes place at –15 °C (Table 3; Entry 10), as indicated by the 0% ee value in the MDB product.

The present stereoselectivity data indicate that the solvent and temperature effects are just confined to the reaction of $^1\text{O}_2$ with *E*-**1**. Both the O_3 and PTAD reactions do not show any noticeable dependence of the stereocontrol on either temperature or solvent. These remarkable stereoselectivity trends require careful mechanistic scrutiny, to understand the details of the enecarbamate oxidation. To enable a detailed comparative mechanistic rationalization of these

trends for the three oxidants $^1\text{O}_2$, O_3 , and PTAD, we will rely on the previously published structural details of the chiral *Z*²⁴ and *E*²⁷ enecarbamates.

4. Discussion

Before entering into a mechanistic analysis of the stereochemical control exercised by $^1\text{O}_2$, O_3 , and PTAD with *Z/E* enecarbamates **1**, the established reaction pathways must be recalled. Both $^1\text{O}_2$ and PTAD approach the alkene double bond (on the XY-plane) perpendicularly (*Z*-axis), as shown in Figure 2 for the transition structures **A** ($^1\text{O}_2$) and **C** (PTAD),^{19–23} whereas O_3 ¹⁸ adds to the double bond laterally, as displayed by the transition structure **B** in Figure 2. Additionally, the major differences and similarities between the three reagents are:

- Both O_3 and PTAD are ground-state molecules and will not experience any excited-state vibrational deactivation as observed for the electronically excited $^1\text{O}_2$; their stereoselectivity is expected to be controlled mainly by steric effects, whereas for $^1\text{O}_2$ also physical quenching may play a role.²⁸
- PTAD^{19–23} is a much larger enophile than $^1\text{O}_2$ and if steric control at the $\text{C}_{3'}$ position is the deciding factor, then a higher stereoselectivity should be expected for PTAD compared to $^1\text{O}_2$.^{14–17}
- O_3 ¹⁸ is similar in size to $^1\text{O}_2$ and should be subject to similar steric interactions,²⁹ but differences may arise from its lateral attack on the double bond versus the perpendicular one for $^1\text{O}_2$.

Based on this mechanistic background, we shall now analyze the factors that underlay the stereoselectivity in the oxidation of both *Z* and *E* enecarbamates with O_3 and PTAD, and compare the present results with our previously published ones^{11,24–27} for $^1\text{O}_2$. A brief summary of the salient features of our experimental data is given below:

- A high stereoselectivity is observed in the formation of MDB for the $^1\text{O}_2$ oxidation of *E*-**1**; whereas a low stereoselectivity is observed for both O_3 and PTAD reactions with *E*-**1**.
- $^1\text{O}_2$ is sensitive to all the stereochemical structural features inherent with the chiral enecarbamate substrate (the alkene *Z/E* geometry, the *R/S* configuration at the C_4 position in the oxazolidinone chiral auxiliary, and the *R/S* configuration at the $\text{C}_{3'}$ position of the

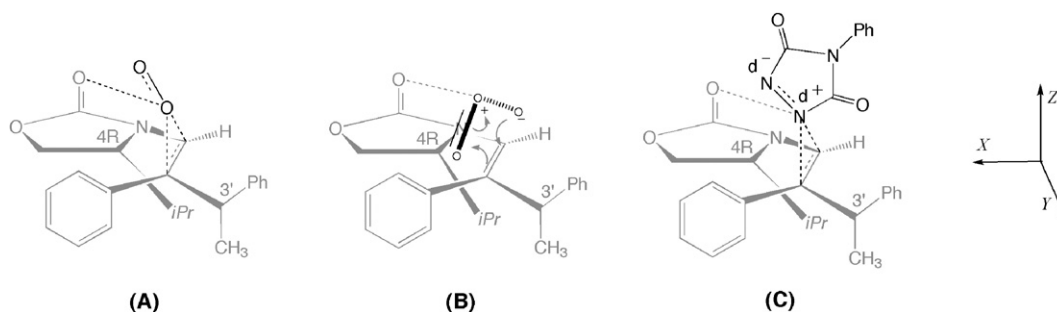


Figure 2. Plausible transition structures for the reactions of $^1\text{O}_2$ (A), O_3 (B), and PTAD (C) with the chiral enecarbamates *Z*-**1**.

phenethyl side chain), as reflected in the vastly different stereoselectivities (Table 3) observed for the *Z* and *E* enecarbamates. This is highlighted by the observation that the photooxidative cleavage of the *E*-1 isomer affords the MDB product in high (up to 97%) enantioselectivity (Table 3), whereas the ee value for the *Z*-1 isomer is low (only 30% at best) under comparable reaction conditions.^{11,24–27} In contrast, both PTAD (Table 1) and O₃ (Table 2), display a very low stereoselectivity for both *Z* and *E* enecarbamates.

- (iii) The sensitivity of the three different reactive species towards C_{3'} stereochemistry follows the order ¹O₂ >> O₃ > PTAD; thus, PTAD reacts preferentially with the C_{3'}(*R*)-epimer irrespective of the alkene *Z/E* geometry, whereas the C_{3'}(*S*)-epimer of the *E* enecarbamate and the C_{3'}(*R*)-epimer of the *Z* enecarbamate are more reactive for O₃.
- (iv) The enantiomeric excess in the MDB product for the ¹O₂ oxidation of the *E*-1 diastereomer depends substantially on the employed solvent and the temperature conditions, but not for the corresponding *Z*-1 enecarbamate (Table 3);^{11,24–27} no significant solvent and temperature effects are evident for the reaction of PTAD (Table 1) and O₃ (Table 2) with both *Z* and *E* enecarbamates.
- (v) Not only does the extent of stereoselection (% ee value) for the *E*-1 diastereomer vary extensively as a function of solvent and temperature (Table 3), but the favored configuration (*R* vs *S* enantiomers of MDB) changes, i.e., there is an inversion in the sense of the stereoselectivity for the ¹O₂ oxidation (Table 3), but not for PTAD (Table 1) or O₃ (Table 2).

This divergent behavior in the stereochemical control displayed by ¹O₂, O₃, and PTAD in their reactivity towards **1** needs to be mechanistically rationalized in terms of the trajectory for the attack on the double bond of the chiral enecarbamate substrate. The configuration at the C_{3'} position is of particular interest in regard to steric blocking (ground-state reactivity) versus vibrational deactivation (excited-state reactivity) by the methyl versus phenyl substituents for attack of the reagent on the double bond.

Since we have employed a 50:50 diastereomeric mixture of enecarbamates *E*-1 (actually, *R/S* epimers at the C_{3'} stereogenic site of the alkyl side chain), the stereoselection in the present case entails *kinetic resolution*.^{11,27} Thus, the enantiomeric excess in the MDB product **3**, which is formed in the double-bond cleavage by ¹O₂ and O₃, reflects the differentiation in the relative reaction rates of the enecarbamate oxidation (Fig. 3). For such *kinetic resolution*, the so-called selectivity factor (*s*),^{35–38} which is a quantitative measure (corrected for the extent of conversion) of the relative reaction rates for the two stereoisomers in question (Eqs. 1 and 2) come to prominence. In the present case, the *s* factor may be computed for the two-epimeric enecarbamates [C_{3'}(*R*) and C_{3'}(*S*) epimers] from the substrate conversion and the MDB enantiomeric excess by using Eqs. 1 and 2. A large *s* value translates to high enantiomeric excess in the MDB product (see Figs. 3 and 4).

For illustration purposes, under identical conditions, the oxidation of *E*(*R*)-1 by ¹O₂ gave an ee value of 97%

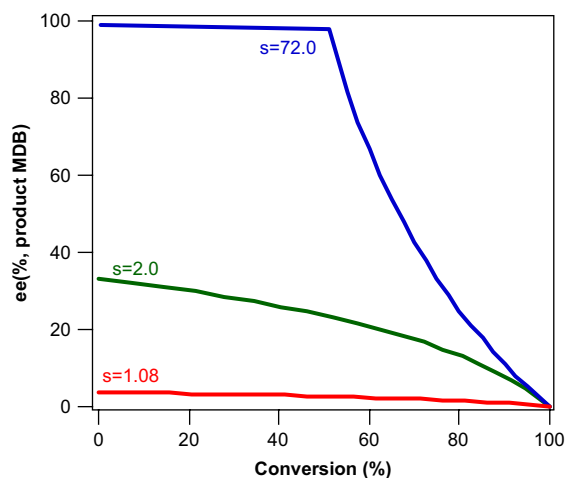


Figure 4. The dependence of the enantiomeric excess of the MDB product on the conversion of the chiral oxazolidinone-functionalized enecarbamates to illustrate the consequences of the difference in the *s* factor.^{35–38}

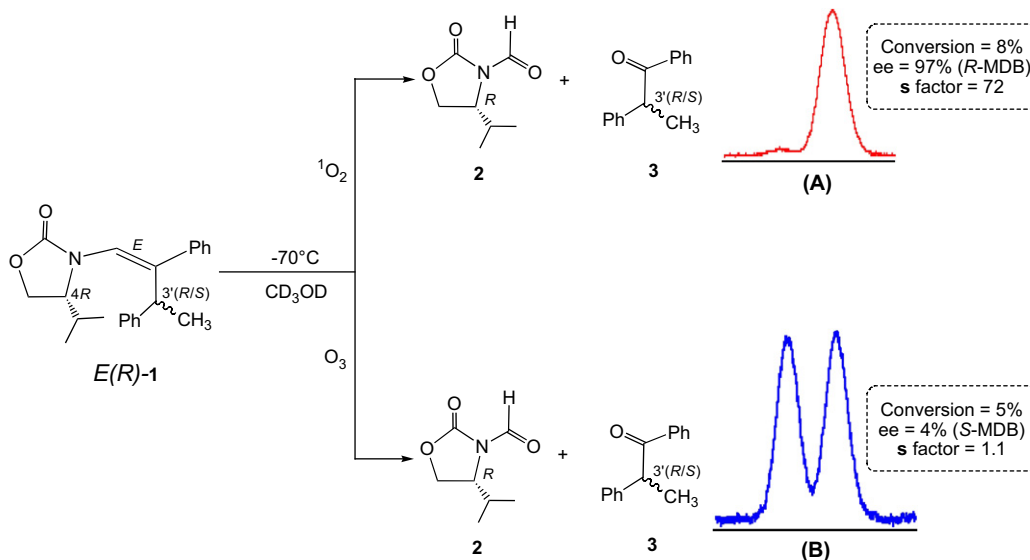


Figure 3. The GC traces of the MDB product for the oxidation of *E*(*R*)-1 by ¹O₂ (A) and O₃ (B) at –70 °C in CD₃OD.

with a s factor of 72, compared to only 4% for the O_3 oxidation with an s factor of about 1.1 (compare Entry 16 in Table 3 and Entry 11 in Table 2). As a practical utilization of such a high s factor in a kinetic resolution, we previously demonstrated¹¹ that we may photochemically resolve the two epimers with 1O_2 by running the photooxygenation of $E(R)$ -1 in CD_3OD at $-70^\circ C$ to nearly 50% conversion. The R -MDB product was separated from the reaction mixture by chromatography and an ee value of 97% was obtained. The unreacted $1'E,4R(iPr),3'S$ -1 encarbamate was then quantitatively photooxidized at room temperature to afford the S -MDB product with an ee value of 97%. This remarkable case of stereoselection for 1O_2 was previously coined as *photochemical Pasteur-type kinetic resolution*.¹¹

The plot of % ee versus conversion in Figure 4 displays that the dependence of the enantioselectivity as a function of conversion for various s factors, as observed for the O_3 oxidation (Table 2), for which the ee values are moderate at low and small at high conversions. For example, 36% ee was observed at 9% conversion and only 4% ee at 36% conversion (Table 2; Entries 20 and 21) for the oxidation of $Z(S)$ -1 by O_3 in CD_2Cl_2 at $-70^\circ C$. The consequence of the difference in the s factors is best illustrated in Figure 3, where an ee value of 97% was obtained for 1O_2 (s factor of 72) compared to an ee value of only 4% for O_3 (s factor of 1.1) in CD_3OD . When stereoselectivity results are rationalized mechanistically in the kinetic-resolution studies, instead of the ee values the s factor should be employed.^{35–38} The reason for this is that the ee value refers to the amount of the enhanced MDB enantiomer uncorrected for the extent of conversion, whereas the s factor reflects the variation in the ee value corrected for the extent of conversion (Eq. 1; Fig. 4).^{35–38} For example, in the case of the O_3 oxidation of $Z(S)$ -1 at $-70^\circ C$, in CD_2Cl_2 the ee value is 4% S -MDB at 36% conversion and the s factor 1.1 (Table 2; Entry 21), while for CD_3OD the ee value is 22% S -MDB at 7% conversion and the s factor 1.6 (Table 2; Entry 28); clearly, there is a large difference in the ee values, but the s factors are almost the same. In the case of the 1O_2 oxidation of the E encarbamate, there is a significant variation in the s factor upon changing the solvent from CD_2Cl_2 (the s factor varies from 2.3 to 40) to CD_3OD (the s factor varies from 7.6 to 72), but not for the Z isomer. Comparison of the stereoselectivity of PTAD, O_3 , and 1O_2 in the various solvents at different temperatures, it is clear that PTAD (Table 1) and O_3 (Table 2), exhibits essentially no temperature effect or solvent effect for both Z/E encarbamates, whereas 1O_2 (Table 3) displays a substantial temperature effect and solvent effect for the E encarbamates and not for the Z encarbamates. The differential activation parameters ($\Delta\Delta S^\ddagger$ and $\Delta\Delta H^\ddagger$) were determined for the reactivity of O_3 and 1O_2 . Since the temperature profile of the stereoselectivity for PTAD is quite similar to that of O_3 , we shall consider only the O_3 and 1O_2 oxidants, but infer for PTAD from the O_3 results. The $\Delta\Delta S^\ddagger$ and $\Delta\Delta H^\ddagger$ values for the 1O_2 and O_3 oxidation of $E(R)$ -1 diastereomer in $CDCl_3$, CD_2Cl_2 , and CD_3OD were computed with the help of the Eyring relation (Eq. 3) and the data are given in Table 2 for O_3 and in Table 3 for 1O_2 .^{2,27,39,40} The $\Delta\Delta S^\ddagger$ and $\Delta\Delta H^\ddagger$ values for the O_3 oxidation of the encarbamate $1 Z/E$ diastereomers reveal a negligible temperature effect in the MDB enantiomeric excess; e.g., the $\Delta\Delta H^\ddagger$ values range

between -0.5 to $+0.6$ kcal mol⁻¹ and the $\Delta\Delta S^\ddagger$ values between -1.0 and $+3.0$ cal mol⁻¹ K⁻¹ over the entire variation of reaction conditions (Table 2). In contrast, a pronounced temperature dependence is displayed for the 1O_2 oxidation, since the $\Delta\Delta H^\ddagger$ term varies between -5.0 and $+5.0$ kcal mol⁻¹ and the $\Delta\Delta S^\ddagger$ term between -17 and $+19$ cal mol⁻¹ K⁻¹ (Table 3). Clearly, the major contribution derived from the differential activation entropy term ($\Delta\Delta S^\ddagger$), in comparison with the differential activation enthalpy term ($\Delta\Delta H^\ddagger$), cannot be ignored.

The experimental trends in the temperature dependence of the enantioselectivity for the O_3 and 1O_2 oxidations of the encarbamates as a function of the solvent nature is given in the Eyring plots for the $E(R)$ -1 diastereomer in Figure 5. The slope of nearly zero in the Eyring plot for the O_3 oxidation in the investigated solvents indicates that this reaction is insensitive to solvent and temperature variations, since the differential activation enthalpy ($\Delta\Delta H^\ddagger$) contributes negligibly.^{41,42} Since the behavior of PTAD parallels that of O_3 , we presume that PTAD also exhibits similar Eyring plots. Also note the nearly parallel lines (similar slopes) for the 1O_2 oxidation, which indicate that the enthalpic contribution ($\Delta\Delta H^\ddagger$) is about the same in the diverse solvents; thus, the stereoselectivity is controlled by the entropic term ($\Delta\Delta S^\ddagger$). Most significant is the crossing of the zero % ee line, which constitutes the inversion point in the sense of the enantioselectivity, i.e., opposite configurations are selected as the favored MDB enantiomer.

The contrasting temperature and solvent dependence of the stereoselectivity observed for the 1O_2 and O_3 reactants (by inference, PTAD is similar to O_3) in their oxidation of the chiral encarbamate substrates is convincingly exposed by the $\Delta\Delta S^\ddagger$ and $\Delta\Delta H^\ddagger$ parameters.^{2,39,40} Thus, the stereoselection is a critical balance of the enthalpy and entropy, which are interrelated by Eqs. 1 and 2. Consequently, the large contribution from the differential activation parameters for the 1O_2 oxidation (Table 3) suggests that the transition state is conformationally flexible and its solvation–desolvation behavior is crucial. Expectedly, the temperature and solvent variations influence the stereo-differentiating step.^{2,39,40} Such entropy effects are indicative of conformational factors,^{2,39,40} which in the present case are dictated, presumably, by the stereogenic center at the $C_{3'}$ position of the phenethyl side chain. In contrast, the low contribution from the differential activation parameters for the O_3 oxidation indicates that the transition state is more rigid and not affected by the variation of the external factors of the system. As expected, there is no significant temperature and solvent dependence in the sense of the stereoselectivity for the O_3 and PTAD oxidations.

These conspicuously complex temperature and solvent effects in the stereoselectivity observed for the oxidation of the E and Z encarbamates by 1O_2 , O_3 , and PTAD can be mechanistically rationalized in terms of the structural features inherent within the chiral substrate and the electronic nature of the oxidants. We previously proposed^{11,24–27} that the high stereocontrol in the photooxidative cleavage of the encarbamates by the electronically excited 1O_2 is the consequence of selective π -facial quenching by the encarbamate substrate. In this context, it is well known that the lifetime of

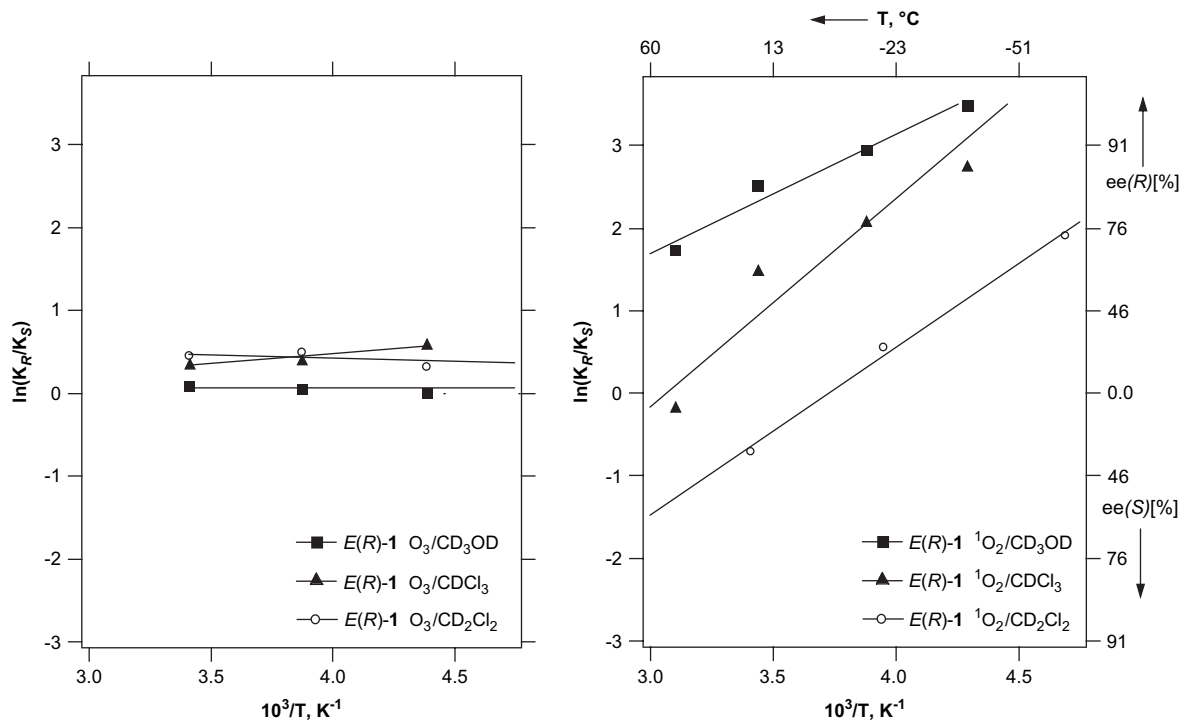


Figure 5. Eyring plots for the stereoselective photooxygenation of *E(R)*-1 by O_3 (left) and 1O_2 (right) in a variety of solvents.

1O_2 in deuterated solvents is much longer than non-deuterated ones,^{14–17} since C–H bond vibrations deactivate 1O_2 to its triplet ground state.²⁸ In view of the higher flexibility of enecarbamates, conformations may be populated, in which one π face of the double bond exposes a larger number of C–H bonds for selective quenching²⁸ of the incoming electronically excited 1O_2 (see Panel A in Fig. 6). Further, deuterium substitution (CD_3 vs CH_3) at the alkene geometry (*cis*- vs *trans*-) in the ene-reaction involving 1O_2 shows a substantial isotope-effect (k_H/k_D for *cis*-: 1.04–1.09 and k_H/k_D for *trans*-: 1.38–1.41).⁴³ If this hypothesis is valid, the ground-state reactive species like PTAD and O_3 will not be vibrationally deactivated like 1O_2 . Thus, for O_3 and PTAD only steric hindrance reflects the observed selectivity. Our analyses of O_3 and PTAD reactivity with the *Z(R)*-1 emphasizes this aspect. As shown in Panel B (O_3) and Panel C (PTAD) of Figure 6, the approach of reactant onto the double bond is hindered from the bottom by the isopropyl group, such that O_3 as well as PTAD are forced to attack from the top. Additionally, kinetic resolution by the stereogenic center at the $C_{3'}$ position of the phenethyl side chain plays a role in enriching one of the MDB enantiomers (Fig. 6).²⁷ For example, in the O_3 oxidation of the 50:50 mixture of the *3'R/S* diastereomers of *Z(R)*-1, the $C_{3'}(R)$ -epimer is more reactive than $C_{3'}(S)$ -epimer, such that the *R*-MDB enantiomer is formed in excess and the $C_{3'}(S)$ -epimer of the *Z* enecarbamate accumulates (see Panel B in Fig. 6). Similar arguments apply also to the reactivity of PTAD with the 50:50 mixture of the *3'R/S* diastereomers of *Z(R)*-1 (see Panel C in Fig. 6), which is corroborated in the observed selectivity (Table 1).

Indeed, if steric effects play a dominant role in the O_3 oxidation, then the observed ee values should be higher when a bulkier ozone-like oxidant is employed in the kinetic resolution of the *R/S* epimers at the $C_{3'}$ position. This expectation was tested with the triphenyl phosphite ozonide

(Scheme 2), which is reported^{44–46} to add at $-70^\circ C$ directly to alkenes through a peroxide-like transition state, i.e., it displays 1O_2 reactivity, but does not involve genuine 1O_2 .

As shown in Scheme 2, an ee value of 83% (*R*-MDB) was observed for the triphenyl phosphite ozonide $[(PhO)_3PO_3]$ oxidation of *Z(R)*-1,^{29,45,46} compared to only 36% (*R*-MDB) for O_3 . Due to the bulkiness of the $(PhO)_3PO_3$ oxidant and its ground-state character, the stereoselectivity displayed in the O_3 (and by inference also PTAD) reactions may be attributed to the steric interference experienced by these reactants with the enecarbamate substrate. Evidently, the much higher stereoselection exhibited by 1O_2 than for O_3 and PTAD suggests that factors other than steric impediments control the stereoselectivity of the 1O_2 oxidations, possibly quenching of the excited state nature of 1O_2 by vibrational interactions.

To understand the intricacies of the complex stereoselectivity trends observed for the 1O_2 , O_3 , and PTAD, the structural characteristics in regard to the stereochemical aspects of the chiral enecarbamates needs to be considered in detail. As shown in Figure 7, the oxazolidinone-functionalized enecarbamate are composed of three distinct stereochemically pertinent structural features, namely the *R/S* configuration at the C_4 position in the oxazolidinone chiral auxiliary, the *Z/E* geometry of the alkenyl double bond (labeled *alkene*), and the *R/S* configuration at the $C_{3'}$ position of the alkyl side chain on the double bond. The following implications on the control of the stereoselectivity imposed by these structural features on the attacking oxidants may be anticipated:

- The reactant may be sterically sensitive to the C_4 position and distinguish between its *R/S* configurations but unable to sense any differences for the *Z/E*

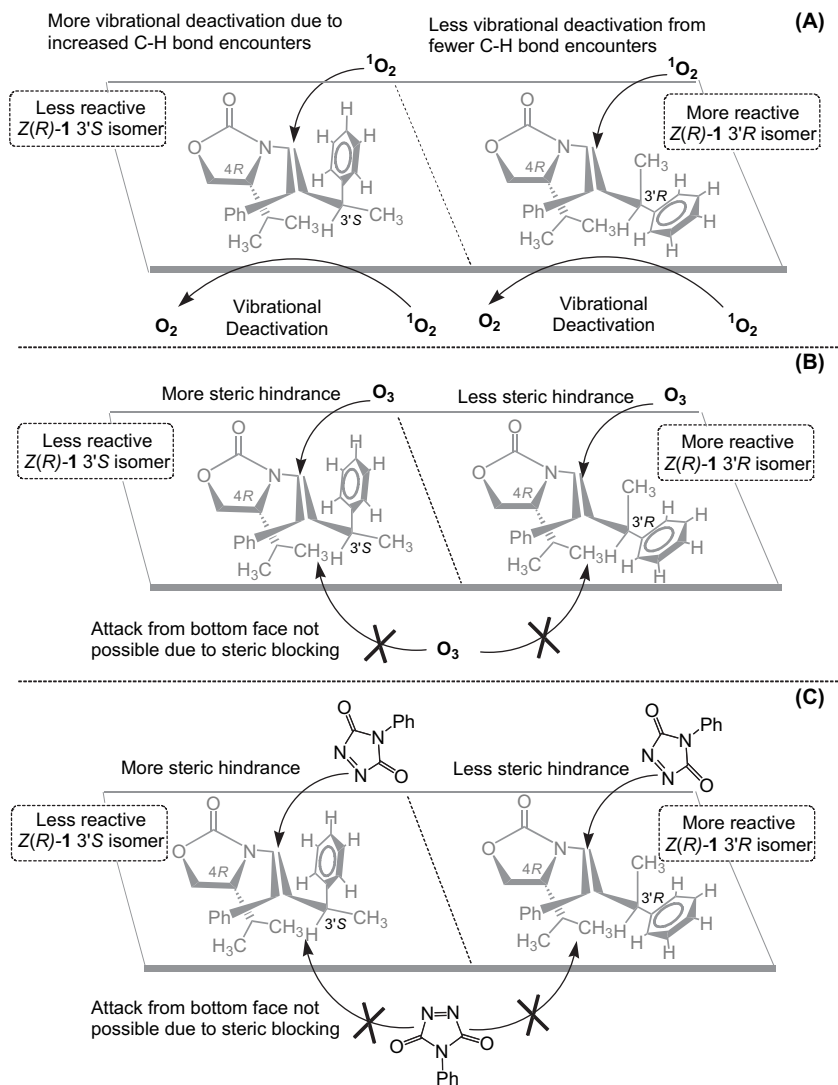
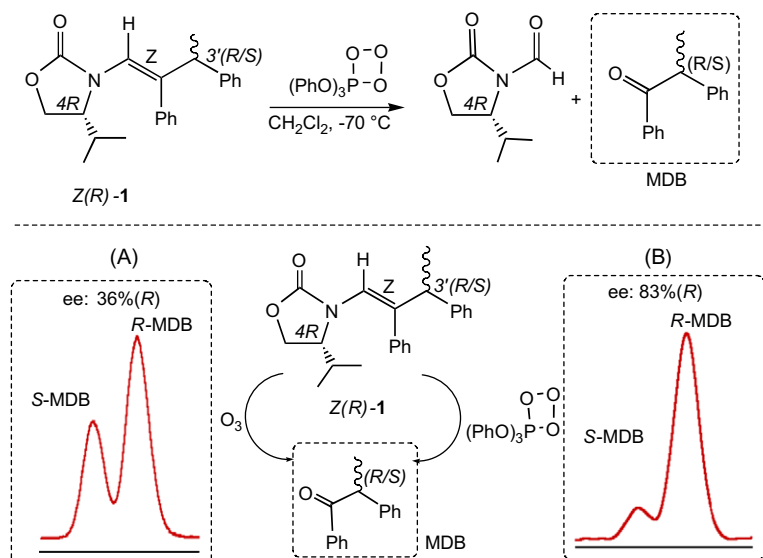


Figure 6. The favored π -facial attack on the alkene double bond of the chiral encarbamate Z(R)-1 by $^1\text{O}_2$ (A), O_3 (B), and PTAD (C).



Scheme 2. Oxidation of the Z(R)-1 diastereomer by O_3 (A) and by $(\text{PhO})_3\text{PO}_3$ (B); for comparison, the corresponding GC traces (chiral stationary phase) are displayed.

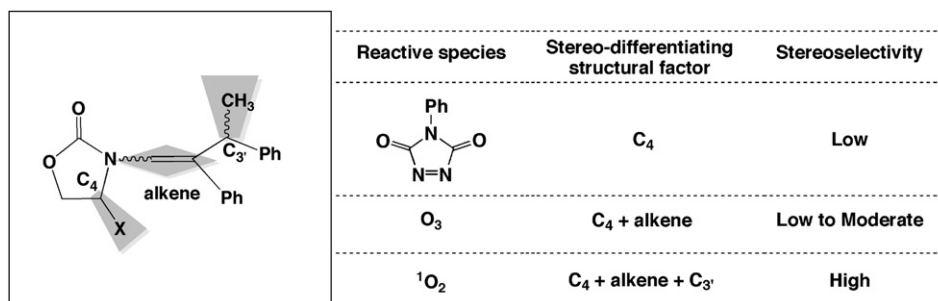


Figure 7. The stereochemically relevant structural composition of the chiral oxazolidinone-functionalized enecarbamates and their implications in regard to stereocontrol.

configurations of the *alkene* geometry nor the *R/S* configurations of the C_{3'} position; a low stereoselectivity should be expected, as displayed by PTAD.

- (ii) The reactant may be sensitive to the C₄ position and the *alkene* geometry, but insensitive to the C_{3'} position; up to a moderate stereoselectivity should be expected, as observed O₃.
- (iii) The reactant may be sensitive to all three stereochemical features, namely the C₄ position, the *alkene* geometry, and the C_{3'} position; a high stereoselectivity should result, as found for ¹O₂.

From the above analysis of the stereochemically relevant structural characteristics of the chiral enecarbamate substrate and the electronic nature of the three reactants, we speculate that the vibrational deactivation (physical quenching) is responsible for the high stereocontrol exhibited by electronically excited ¹O₂ (~97% ee at -70 °C; CD₃OD, Table 2).²⁸ In contrast, the ground-state O₃ and PTAD oxidants are only subject to classical steric effects, which are relatively ineffective for stereoselection. Thus, the product-generating chemical pathway competes with the physical quenching process through vibrational deactivation by C–H bonds.^{28,47} In the vibrational deactivation scenario, the isopropyl group at the C₄ position of the oxazolidinone chiral auxiliary is apparently responsible for the excited-state deactivation of ¹O₂. To compare directly the influence of vibrational deactivation encountered in [2+2] cycloaddition with that of ene reaction should be of pertinent mechanistic interest. In our case, such comparison with the same substrates will not be possible as the phenethyl group exclusively gives the [2+2] cycloaddition product. The phenethyl group would need to be replaced with a methyl group, to study the influence of vibrational deactivation for the ene reaction. Previously we have demonstrated that the oxazolidinone chiral auxiliary provides high π -facial selectivity through the C₄ substituent for both the ene and the [2+2] reaction in the case of substrates that have the methyl instead of the phenethyl group.²⁵ It was also shown that the mode selectivity (*ene* vs [2+2]) depends on the *alkene E* versus *Z* geometry, which was explained in terms of an orbital-directing effect of the enamine-type functionality.²⁵ Again, deuterated substrates would be necessary to examine the influence of vibrational deactivation in the ene reaction. A promising mechanistic probe to validate this novel phenomenon of stereoselective quenching of ¹O₂, involves the deuteration of the alkyl substituents at the C₄ and C_{3'} stereogenic centers. Such studies are in progress in our laboratory.

5. Conclusion

The current comparative study involving ¹O₂, O₃, and PTAD with enecarbamates **1** provides detailed insights into the intricate nature of the steric and electronic interactions required to achieve a high selectivity in the photooxygenation of chiral alkenes. The extensive stereochemically relevant structural properties embodied in the chiral oxazolidinone-substituted enecarbamates (i.e., the chiral centers at the C₄ position of the oxazolidinone ring and at the C_{3'} position of the phenethyl side chain, as well as the *E/Z* configurations of the *alkene* functionality) make these substrates informative molecular probes to explore the mechanistic intricacies of the oxidative cleavage of alkenyl double bonds. The stereoselection depends not only on the *alkene* geometry (*Z/E*), the size of the C₄ alkyl substituent (*H*, *Me*, *iPr*) in the oxazolidinone ring, the configuration (*R/S*) at the C_{3'} stereogenic center of the phenethyl side chain, the solvent, and temperature, but also on the electronic nature (excited vs ground state) of the oxidant. The most dramatic effects on the stereocontrol have been seen for the conformationally more flexible *E* diastereomer, which responds to the electronic characteristics of the reactive species, possibly through the selective vibrational quenching by the substituents at the C_{3'} position of the chiral enecarbamates as a function of their configuration. The stereochemical consequence of this novel phenomenon deserves further exploration in photochemical transformations.

Acknowledgements

The authors at Columbia thank the NSF (CHE 01-10655 and CHE-04-15516) for generous support of this research. W.A. is grateful for the financial support from the Deutsche Forschungsgemeinschaft, Alexander-von-Humboldt Stiftung, the Fonds der Chemischen Industrie, and the hospitality of the University of Puerto Rico. T.P. acknowledges the support of the W.M. Keck Foundation. H.S. and Y.I. gratefully acknowledge a JSPS research fellowship for young scientists (08384). The oxidative work with ¹O₂ and O₃ was carried out at the Columbia University, and the PTAD studies were conducted at Claremont McKenna, Pitzer, and Scripps Colleges.

References and notes

- Chiral Photochemistry*; Inoue, Y., Ramamurthy, V., Eds.; Marcel Decker: New York, NY, 2004.
- Inoue, Y. *Chem. Rev.* **1992**, *92*, 741–770.

3. Rau, H. *Chem. Rev.* **1983**, *83*, 535–547.
4. Turro, N. J. *Proc. Natl. Acad. Sci. U.S.A.* **2002**, *99*, 4805–4809.
5. Turro, N. J.; Cheng, C. C.; Abrams, L.; Corbin, D. R. *J. Am. Chem. Soc.* **1987**, *109*, 2449–2456.
6. *Photochemistry in Organized and Constrained Media*; Ramamurthy, V., Ed.; Wiley-VCH: New York, NY, 1991.
7. Garcia-Garibay, M. A. *Acc. Chem. Res.* **2003**, *36*, 491–498.
8. Sivaguru, J.; Natarajan, A.; Kaanumalle, L. S.; Shailaja, J.; Uppili, S.; Joy, A.; Ramamurthy, V. *Acc. Chem. Res.* **2003**, *36*, 509–521.
9. Sivaguru, J.; Shailaja, J.; Uppili, S.; Ponchot, K.; Joy, A.; Arunkumar, N.; Ramamurthy, V. Achieving Enantio and Diastereoselectivities in Photoreactions Through the Use of a Confined Space. In *Organic Solid-State Reactions*; Toda, F., Ed.; Kluwer Academic: Dordrecht, The Netherlands, 2002; pp 159–188.
10. Poon, T.; Turro, N. J.; Chapman, J.; Lakshminarasimhan, P.; Lei, X.; Adam, W.; Bosio, S. G. *Org. Lett.* **2003**, *5*, 2025–2028.
11. Poon, T.; Sivaguru, J.; Franz, R.; Jockusch, S.; Martinez, C.; Washington, I.; Adam, W.; Inoue, Y.; Turro, N. J. *J. Am. Chem. Soc.* **2004**, *126*, 10498–10499.
12. Sivaguru, J.; Poon, T.; Franz, R.; Jockusch, S.; Adam, W.; Turro, N. J. *J. Am. Chem. Soc.* **2004**, *126*, 10816–10817.
13. Singlet Oxygen Feat. *Chem. Eng. News* **2004**, *82*, 7.
14. *Singlet Oxygen*; Wasserman, H. H., Murray, R. W., Eds.; Academic: New York, NY, 1979.
15. Gollnick, K.; Kuhn, H. J. *Singlet Oxygen*; Wasserman, H. H., Murray, R. W., Eds.; Academic: New York, NY, 1979.
16. Foote, C. S. *Acc. Chem. Res.* **1968**, *1*, 104–110.
17. *Singlet Oxygen*; Frimer, A. A., Ed.; CRC: Boca Raton, 1985; Vols. 1–4.
18. Bailey, P. S. *Ozonation in Organic Chemistry*; Academic: New York, NY, 1978; Vols. 1–2.
19. Adam, W.; De Lucchi, O. *Tetrahedron Lett.* **1981**, *22*, 929–932.
20. Adam, W.; Schwarm, M. *J. Org. Chem.* **1988**, *53*, 3129–3130.
21. Adam, W.; Bottke, N.; Krebs, O. *J. Am. Chem. Soc.* **2000**, *122*, 6791–6792.
22. Adam, W.; Bottke, N.; Krebs, O. *Org. Lett.* **2000**, *21*, 3293–3296.
23. Leach, A. G.; Houk, K. N. *Chem. Commun.* **2002**, 1243–1255.
24. Adam, W.; Bosio, S. G.; Turro, N. J.; Wolff, B. T. *J. Org. Chem.* **2004**, *69*, 1704–1715.
25. Adam, W.; Bosio, S. G.; Turro, N. J. *J. Am. Chem. Soc.* **2002**, *124*, 14004–14005.
26. Adam, W.; Bosio, S. G.; Turro, N. J. *J. Am. Chem. Soc.* **2002**, *124*, 8814–8815.
27. Sivaguru, J.; Solomon, M. R.; Saito, H.; Poon, T.; Jockusch, S.; Adam, W.; Inoue, Y.; Turro, N. J. *Tetrahedron* **2006**, *62*, 6707–6717.
28. Turro, N. J. *Tetrahedron* **1985**, *41*, 2089–2098.
29. Sivaguru, J.; Saito, H.; Poon, T.; Omonuwa, T.; Franz, R.; Jockusch, S.; Hooper, C.; Inoue, Y.; Adam, W.; Turro, N. J. *Org. Lett.* **2005**, *7*, 2089–2092.
30. Greenwodd, F. L. *J. Org. Chem.* **1945**, *10*, 414–418.
31. Evans, D. A.; Bartroli, J.; Shih, T. L. *J. Am. Chem. Soc.* **1981**, *103*, 2127–2129.
32. Ager, D. J.; Prakash, I.; Schaad, D. R. *Chem. Rev.* **1996**, *96*, 835–876.
33. Evans, D. A.; Chapman, K. T.; Hung, D. T.; Kawaguchi, A. T. *Angew. Chem., Int. Ed. Engl.* **1987**, *26*, 1184–1186.
34. Saito, H.; Sivaguru, J.; Jockusch, S.; Inoue, Y.; Adam, W.; Turro, N. J. *Chem. Commun.* **2005**, 3424–3426.
35. Kagan, H. B.; Fiaud, J. C. *Top. Stereochem.* **1988**, *18*, 249–330.
36. Keith, J. M.; Larrow, J. F.; Jacobsen, E. N. *Adv. Synth. Catal.* **2001**, *343*, 5–26.
37. Martin, V. S.; Woodward, S. S.; Katsuki, T.; Yamada, Y.; Ikeda, M.; Sharpless, K. B. *J. Am. Chem. Soc.* **1981**, *103*, 6237–6240.
38. Chen, C. S.; Fujimoto, Y.; Girdaukas, G.; Sih, C. J. *J. Am. Chem. Soc.* **1982**, *104*, 7294–7299.
39. Buschmann, H.; Scharf, H.-D.; Hoffmann, N.; Esser, P. *Angew. Chem., Int. Ed. Engl.* **1991**, *30*, 477–515.
40. Otera, J.; Sakamoto, K.; Tsukamoto, T.; Orita, A. *Tetrahedron Lett.* **1998**, *39*, 3201–3204.
41. Leffler, J. E. *J. Org. Chem.* **1966**, *31*, 533–537.
42. Leffler, J. E. *J. Org. Chem.* **1955**, *20*, 1202–1231.
43. Grdina, B. M.; Orfanopoulos, M.; Stephenson, L. M. *J. Am. Chem. Soc.* **1979**, *101*, 3111–3112.
44. Above $-30\text{ }^{\circ}\text{C}$, the ozonide liberates $^1\text{O}_2$ while at lower temperatures, the ozonide itself is an oxidant.
45. Mori, A.; Abe, M.; Nojima, M. *J. Org. Chem.* **2001**, *66*, 3548–3553.
46. Stephenson, L. M.; Zielinski, M. B. *J. Am. Chem. Soc.* **1982**, *104*, 5819–5820.
47. Poon, T.; Turro, N. J.; Chapman, J.; Lakshminarasimhan, P.; Lei, X.; Jockusch, S.; Franz, R.; Washington, I.; Adam, W.; Bosio, S. G. *Org. Lett.* **2003**, *5*, 4951–4953.